

**Seawater Density Variations in the North Atlantic and the Atlantic  
Meridional Overturning Circulation**

Chunzai Wang<sup>1</sup>

Shenfu Dong<sup>2</sup>

Ernesto Munoz<sup>2</sup>

<sup>1</sup> NOAA Atlantic Oceanographic and Meteorological Laboratory  
Miami, Florida

<sup>2</sup> Cooperative Institute for Marine and Atmospheric Studies  
University of Miami  
Miami, Florida

Revised to *Climate Dynamics*

March 2009

Corresponding author address: Dr. Chunzai Wang, Physical Oceanography Division,  
NOAA/AOML, 4301 Rickenbacker Causeway, Miami, FL 33149, USA.  
E-mail: Chunzai.Wang@noaa.gov.

## **Abstract**

Seawater property changes in the North Atlantic Ocean affect the Atlantic meridional overturning circulation (AMOC), which transports warm water northward from the upper ocean and contributes to the temperate climate of Europe, as well as influences climate globally. Previous observational studies have focused on salinity and freshwater variability in the sinking region of the North Atlantic, since it is believed that a freshening North Atlantic basin can slow down or halt the flow of the AMOC. Here we use available data to show the importance of how density patterns over the upper ocean of the North Atlantic affect the strength of the AMOC. For the long-term trend, the upper ocean of the subpolar North Atlantic is becoming cooler and fresher, whereas the subtropical North Atlantic is becoming warmer and saltier. On a multidecadal timescale, the upper ocean of the North Atlantic has generally been warmer and saltier since 1995. The heat and salt content in the subpolar North Atlantic lags that in the subtropical North Atlantic by about 8-9 years, suggesting a lower latitude origin for the temperature and salinity anomalies. Because of the opposite effects of temperature and salinity on density for both long-term trend and multidecadal timescales, these variations do not result in a density reduction in the subpolar North Atlantic for slowing down the AMOC. Indeed, the variations in the meridional density gradient between the subpolar and subtropical North Atlantic Ocean suggest that the AMOC may have become stronger over the past five decades. These observed results are supported by and consistent with some oceanic reanalysis products.

## 1. Introduction

The North Atlantic Ocean is a critical region for the Atlantic meridional overturning circulation (AMOC) since its variability can change seawater properties in the North Atlantic regions of deep-water formation and thus affects the strength of the AMOC. The AMOC, through its northward transport of warm tropical waters by the Gulf Stream and North Atlantic Current, effectively contributes to the temperate climate of Europe, as well as influences climate globally (e.g., Vellinga and Wood 2002; Dong and Sutton 2002; Timmermann et al. 2007; Schmittner et al. 2007). In addition, the North Atlantic also hosts a climate phenomenon known as the Atlantic multidecadal oscillation (AMO), a fluctuating climate mode wherein the sea surface temperature (SST) can vary on multidecadal timescales of 30-80 years with the largest variations centered in the high latitudes of the North Atlantic (e.g., Delworth and Mann 2000; Enfield et al. 2001; Wang et al. 2008a). It is shown that the AMOC is a driving mechanism for the AMO (e.g., Delworth and Mann 2000; Knight et al. 2005; Dijkstra et al. 2006; Zhang et al. 2007). The SST variability of the AMO is associated with changes of climate and extreme weather events such as rainfall and drought/flood in North America and Atlantic hurricane activity (e.g., Enfield et al. 2001; McCabe et al. 2004; Goldenberg et al. 2001; Bell and Chelliah 2006; Wang et al. 2008a). Thus, improving our understanding of North Atlantic variability is very important both scientifically and socially.

There are many papers in the literature that examine variability in the North Atlantic Ocean. For observational studies of the AMO, focuses are mainly on SST variability probably owing to its relatively long record that is required for a multidecadal timescale study. For observational studies related to the AMOC, attentions are paid to salinity and freshwater variability in the sinking region of the North Atlantic (e.g., Dickson et al. 2002; Curry et al.

2003; Boyer et al. 2007), since it is believed that a freshening North Atlantic basin can slow down or halt the flow of the AMOC. For example, Dickson et al. (2002) have reported by using hydrographic records that the high latitudes of the North Atlantic gradually become fresher during the past decades. Curry et al. (2003) have examined salinity and temperature difference between the periods of 1985-99 and 1955-69. However, Curry et al.'s approach could not show the AMO signal since the period of 1985-99 covers both the positive and negative phases of the AMO. In addition, we should keep in mind that the ocean meridional overturning circulation is density-driven. The density of seawater is determined by both salinity and temperature. The saltier the denser, and the warmer the lighter. Saltier water is denser than fresher water because the dissolved salts fill interstices between water molecules, resulting in more mass per unit volume. Warmer seawater expands and is thus less dense than cooler seawater. It thus seems that the analyses of salinity, temperature and density variability in the North Atlantic are necessary for us to understand the AMOC.

The purpose of the present paper is to analyze available oceanic data in the North Atlantic Ocean during the past decades. This paper makes several contributions. First, we calculate potential density from the available salinity and temperature data, and then analyze co-variability of salinity, temperature and density on timescales of the long-term trend (related to global warming) and multidecadal variation (i.e., the AMO). Second, we show different features of North Atlantic Ocean variability on the long-term trend and multidecadal timescales, and quantify the salinity and temperature contributions to potential density variability in the upper ocean of the North Atlantic. Third, we show that the AMO signal can reach deeper than just SST manifestation (previous observational studies have focused on the AMO using SST data) and the AMO signal is also manifested in the upper ocean salinity of the North Atlantic. Fourth, we

observe that the temperature and salinity anomalies in the subpolar North Atlantic Ocean lag those in the subtropical North Atlantic Ocean by about 8-9 years. Fifth, we show with assistance of oceanic reanalysis products that the strength of the AMOC may be related to the meridional density gradient between the subpolar and subtropical North Atlantic Ocean, and that the AMOC may have strengthened during the past decades.

The paper is organized as follows. Section 2 describes the data sets, oceanic reanalysis products (or oceanic model data) and methods used in this study. Section 3 shows the mean states of the North Atlantic Ocean. Sections 4 and 5 show variability of temperature, salinity and density in the North Atlantic Ocean for the long-term trend and multidecadal timescales, respectively. Section 6 discusses the relationship between the AMOC and the meridional density gradient between the subpolar and subtropical North Atlantic Ocean. Section 7 provides a summary and discussion.

## **2. Datasets, reanalysis products and methods**

The temperature and salinity dataset is the World Ocean Database 2005 from the National Oceanographic Data Center (Boyer et al. 2005 and 2006), which contains the data in the World Ocean Database 2001 (Conkright et al. 2002) plus the data collected afterwards. The temperature data has two parts: one is the annual mean and the other one is anomaly. The temperature anomaly is calculated by subtracting the appropriate monthly temperature climatology from each temperature profile and then performing an objective mapping and a yearly average. The yearly temperature data covers the period from 1955-2003 and its horizontal resolution is on a  $1.0^{\circ} \times 1.0^{\circ}$  latitude-longitude grid. The yearly temperature data is over the upper ocean from the sea surface to 700 m at standard depth levels of 0, 10, 20, 30, 50, 75, 100,

125, 150, 200, 250, 300, 400, 500, 600, and 700 m. Due to the non-uniform vertical grid, a layer thickness weighted average is performed when data are averaged over depths of 0-700 m.

The salinity data also has two parts: the annual mean and anomaly fields. The anomaly is pentadal for the periods 1955-1959 to 2002-2006. Assigning the time to be the center of each 5-year window, we can obtain the salinity anomaly field covering from 1957 to 2004. Both the mean and anomalous salinity fields are on a  $1.0^{\circ} \times 1.0^{\circ}$  latitude-longitude grid at standard depth levels from the sea surface to 3000 m. To consider co-variability of temperature and salinity fields, we choose the study period from 1957-2003 and the upper ocean of the North Atlantic from the sea surface to 700 m.

Three ocean reanalysis products are also used in this study: the Simple Ocean Data Assimilation (SODA) (Carton and Giese 2008), the German Estimating the Circulation and Climate of the Ocean (GECCO) (Kohl et al. 2006), and the Geophysical Fluid Dynamics Laboratory (GFDL) (Rosati et al. 2004). The SODA uses an ocean general circulation model to assimilate available temperature and salinity observations. The product is a gridded dataset of oceanic variables with monthly values at a  $0.5^{\circ} \times 0.5^{\circ}$  latitude-longitude horizontal resolution and 40 vertical levels. The version 2.0.2 of the SODA is used, with the temperature, salinity and meridional ocean velocity covering from 1958 to 2005. Since the SODA product does not have the density field, we use temperature and salinity fields to calculate potential density relative to the sea surface. The GECCO is also a monthly product from 1952 to 2001, with a  $1.0^{\circ} \times 1.0^{\circ}$  latitude-longitude horizontal resolution and 23 vertical levels. The GFDL ocean product is from 1960 to 2004, with a  $1.0^{\circ} \times 1.0^{\circ}$  latitude-longitude horizontal resolution (enhanced to  $1/3^{\circ} \times 1/3^{\circ}$  in the tropics between  $30^{\circ}\text{S}$  and  $30^{\circ}\text{N}$ ) and 50 vertical levels.

Another dataset used in this study is evaporation minus precipitation (E-P) from the

Southampton Oceanography Center freshwater flux climatology version 1.1. The climatological data is determined from *in situ* meteorological reports in the Comprehensive Ocean Atmosphere Dataset (COAD) covering the period of 1980-1993 (Josey et al. 1998). Both evaporation and precipitation rates are on a  $1.0^\circ \times 1.0^\circ$  latitude-longitude grid.

Given the salinity and temperature data, we can calculate potential density  $\sigma_\theta$ . Total (mean + anomaly) salinity and temperature data were used to compute potential density relative to the sea surface at each grid point for the period 1957-2003. SEAWATER, a computational routine for calculating potential density, is used to determine total potential density. The routine is based on Gill (1982) and is developed by Australia's Commonwealth Scientific and Industrial Research Organization. The mean and anomalous potential densities are then calculated based on the total density from 1957-2003.

In this paper, we also estimate the relative contributions of salinity and temperature fluctuations to potential density variability. Salinity contributions are calculated by using the mean temperature and total salinity fields, whereas temperature contributions are calculated by using the total temperature and mean salinity fields. Mathematically, we separate the potential density variability ( $\Delta\sigma_\theta$ ) into the contributions made by both salinity ( $\Delta\sigma_\theta^S$ ) and temperature ( $\Delta\sigma_\theta^T$ ) fluctuations:

$$\Delta\sigma_\theta = (\partial\sigma_\theta / \partial S)\Delta S + (\partial\sigma_\theta / \partial T)\Delta T \equiv \Delta\sigma_\theta^S + \Delta\sigma_\theta^T. \quad (1)$$

As a traditional way to examine the AMOC, we calculate the streamfunction of the AMOC from ocean velocity distribution. In this paper, the streamfunction of the AMOC is calculated from the meridional velocity  $v(x, y, z, t)$  of the ocean reanalysis products as:

$$\psi(y, z, t) = \int_{-H}^{-z} \int_{X_{WEST}}^{X_{EAST}} v(x, y, z, t) dx dz, \quad (2)$$

where  $H$  is the sea bottom,  $X_{WEST}$  is the ocean western boundary, and  $X_{EAST}$  is the ocean eastern boundary.

### 3. Mean states

Before we examine the long-term trend and multidecadal variations, we first discuss the seawater properties of mean states in the upper ocean of the North Atlantic. Figure 1 shows the annual mean E-P, sea surface salinity (SSS), SST and surface potential density in the North Atlantic. Underlying the easterly trade wind belt at the south edge of the North Atlantic subtropical high, the maximum of E-P is stretched from the eastern subtropical basin west of the African continent to the western tropical North Atlantic and then to the Caribbean Sea, the Gulf of Mexico, and the U.S. southeastern seaboard. The minimum of E-P is associated with the Atlantic intertropical convergence zone (ITCZ) because of a large precipitation and a small wind speed near the center of the ITCZ. Fresh water is transported as atmospheric water vapor from the low to high latitudes where it enters the ocean as precipitation and continental runoff, and evaporation is decreased poleward. In consequence, the second minimum of E-P is located in the high latitudes of the subpolar North Atlantic (Fig. 1a). Consistent with the maximum of E-P, the maximum SSS is resided in the subtropical North Atlantic between 15°N-40°N (Fig. 1b). The SSS is relatively low in the ITCZ region and the subpolar North Atlantic. In general, the surface seawater is warm in the tropical and subtropical North Atlantic, and cold in the subpolar North Atlantic because of the poleward decrease in solar radiation. Given the distribution of SSS and SST in the North Atlantic, surface potential density is large in the high latitudes and decreases toward the tropics with a minimum density belt extended from the eastern ITCZ region to the region of the Atlantic warm pool (i.e., the western tropical North Atlantic, the Caribbean

Sea and the Gulf of Mexico) (Fig. 1d).

The above features of salinity, temperature and density are not limited to the sea surface only. The zonally-averaged annual mean salinity, temperature and potential density as a function of depth and latitude are shown in Fig. 2. The latitudinal variation of SSS can penetrate deeply. In particular, the relative maximum salinity in the subtropical North Atlantic is manifested in the upper layer of 700 m, despite the maximum value being in the upper 250 m (Fig. 2a). In comparison with that in the tropical region, the seawater temperature in the subpolar North Atlantic is relatively uniform in the vertical direction (Fig. 2b). This reflects the fact that the cool water due to the heat loss (to the atmosphere) in the high latitudes can sink and induce oceanic convection (This is also a reason why the AMOC exists in the Atlantic). In other words, the deep penetration of the surface temperature signal in the subpolar North Atlantic sinking region is clearly visible in Fig. 2b. Another feature in Fig. 2b is that the meridional ocean temperature gradient is large north of 30°N, consistent with the geostrophic balance of the eastward Gulf Stream and North Atlantic current. Figure 2c shows that the potential density in the North Atlantic increases with latitude and depth, a conventional large-scale property distribution of seawater.

The spatial distributions of the mean salinity, temperature and potential density averaged over depths of 0-700 m are shown in Fig. 3. Their patterns are generally similar to those at the sea surface as shown in Fig. 1. However, several differences are worthy mentioning here. First, unlike SST (which is maximized in the tropical region), the upper ocean temperature shows a maximum in the subtropical North Atlantic (Fig. 3b), reflecting that the warm surface water penetrates deeper around 30°N (Fig. 2b). Second, unlike at the sea surface, the ITCZ is not obvious in the upper ocean salinity, temperature and potential density. This indicates that

surface seawater property related to the ITCZ is shallow and does not penetrate deeper (see Fig. 2). Third, low (high) potential density in the upper ocean of the subtropical (subpolar) North Atlantic is accompanied by the warm (cold) and high (low) salinity seawater in the subtropical (subpolar) North Atlantic (Figs. 3a-c). These low/high patterns of seawater property in the North Atlantic basically reflect upper ocean circulation of the subtropical and subpolar gyres.

#### **4. Long-term trends**

The long-term linear trend spatial patterns of temperature and salinity anomalies averaged over depths of 0-700 m are shown in Fig. 4. The upper ocean of the tropical and subtropical North Atlantic becomes warm and salty, whereas the subpolar North Atlantic basin is secularly cooled and freshened. Both the warming and increased salinity are maximized in the Gulf Stream region, indicating a large and long-term variation in the Gulf Stream. Although the mechanisms of the secular warming and cooling need to be further studied, the warming may be consistent with expected effects of an increase in greenhouse gas concentrations and the cooling may be suggestive of radiative effects of aerosols and/or oceanic natural variability (e.g., Santer et al. 2006; Mann and Emanuel 2006; Hegerl et al. 2007). The salinity trends may result from many processes such as evaporation, precipitation, ocean circulation and ice melting in the Nordic Seas. However, the mechanism study of the temperature and salinity trend patterns in the North Atlantic is beyond the scope of the present paper.

Given the long-term trend patterns of temperature and salinity anomalies, Fig. 5a shows the trend of potential density anomalies averaged over depths of 0-700 m. The main feature is that the potential density in the subtropical North Atlantic is secularly decreased (i.e., the seawater becomes lighter) and the density trend in the subpolar North Atlantic is relatively small.

Since potential density is determined by both temperature and salinity, we separate the potential density trend into the contributions by temperature and salinity trends. Figures 5b and 5c show that the potential density trends resulting from the temperature and salinity trends are opposite. In the subtropical North Atlantic, warming trend decreases the potential density (Fig. 5b), whereas greater salinity trend increases the density (Fig. 5c). Since the warming-induced effect is larger than that induced by salinity, the net result is a decrease of the potential density in the subtropical North Atlantic (Fig. 5a). However, in the subpolar North Atlantic, cooling trend increases the density and freshening trend decreases the density. The amplitudes of the increased and decreased density are in a similar order, thus resulting in a small value for the potential density trend in the subpolar North Atlantic (Fig. 5a).

The zonally-averaged trends of temperature and salinity anomalies as a function of depth and latitude are shown in Fig. 6. The trends do not change sign vertically over almost all latitudes. The freshening in the subpolar North Atlantic can reach to a depth of 700 m, whereas increased salinity in the tropical and subtropical Atlantic is mainly limited to the upper layer of 200 m (Fig. 6b). This may reflect oceanic convective activity in the North Atlantic sinking region at the higher latitudes. Figure 6a shows an upper layer warming north of 75°N, indicating that the Nordic Seas and Arctic Ocean become warmer associated with global warming. Figure 7 shows the zonally-averaged trends of the potential density anomalies and the potential density trend contributions by temperature and salinity trends. The opposite or compensating effect of temperature and salinity trends on density trend is clearly seen in Figs. 7b and 7c. Again, the compensating effect of temperature and salinity trends on the potential density trend makes the potential density trend in the subpolar North Atlantic small. The large decreasing trend of potential density around 40°N in the upper 700 m reflects the warming-induced density effect in

the regions of the Gulf Stream and its eastward extension (Figs. 6a and 7b).

## **5. Multidecadal variability**

To clearly show the multidecadal signal, we first remove the linear trend from the anomaly data at all grids and depths before the AMO analyses. Previous studies show that the AMO is an oscillatory mode occurring in the North Atlantic SST with its largest variation centered in the high latitudes of the North Atlantic (e.g., Delworth and Mann 2000; Enfield et al. 2001; McCabe et al. 2004; Gray et al. 2004; Wang et al. 2008a). To our knowledge, how the salinity, density and temperature in the upper ocean of the North Atlantic vary with the AMO is not documented previously. Figure 8 shows the time series of temperature, salinity and potential density anomalies in the subpolar North Atlantic of 50°N-75°N, 60°W-10°E averaged over depths of 0-700 m. In addition to SST (as shown previously, North Atlantic SST is cool during 1970-1994, and warm before 1970 and after 1995), the AMO signal is also manifested in the upper ocean temperature of the subpolar North Atlantic. Interestingly, the salinity anomalies in the upper ocean of the subpolar North Atlantic also vary with the AMO (Fig. 8a). The upper ocean of the subpolar North Atlantic is cooler and fresher during the cool phase of the AMO (1970-1990), whereas it is warmer and saltier during the warm phases of the AMO (before 1970 and after 1995). These observed features of temperature and salinity support the hypothesis that the driving mechanism of the AMO involves fluctuations of the AMOC (e.g., Delworth and Mann 2000; Knight et al. 2005; Dijkstra et al. 2006). As the AMOC is enhanced, an increase in heat and salinity occurs in the subpolar ocean owing to the northward transport of heat and salt from the subtropical ocean (as shown in the mean states of Figs. 1-3, seawater is warm and salty in the subtropical North Atlantic Ocean). A reduction of the AMOC would result in the reverse

scenario.

However, the potential density anomalies in the upper ocean of the subpolar North Atlantic do not precisely coincide with the AMO (Fig. 8b). This occurs because potential density is dependent on both temperature and salinity. As shown in Fig. 8c, potential density contributions from temperature and salinity variations are all indicative of the AMO signal. Warmer (cooler) ocean temperature during the warm (cool) phase of the AMO decreases (increases) potential density, whereas higher (lower) level of salinity during the warm (cool) phase of the AMO enhances (reduces) potential density. These opposite effects determine the variation of the potential density anomalies in the subpolar North Atlantic. The competition between temperature and salinity fluctuations causes the potential density anomalies to differ from the AMO, although both the temperature and salinity anomalies vary with the AMO. Another feature in Figure 8 is that the potential density anomalies follow the contribution by temperature more closely than that by salinity, indicating that the density of seawater is more influenced by temperature in the upper ocean of the subpolar North Atlantic.

To examine horizontal and vertical structures in the upper ocean of the North Atlantic associated with the AMO, we choose the eight-year period from 1996-2003 for the positive AMO phase and the eight-year period from 1976-1983 for the negative AMO phase. Figure 9 shows the temperature and salinity anomaly (averaged over depths of 0-700 m) difference between the eight years of positive and negative AMO phases. We also examine the positive and negative AMO phases separately and find that their anomaly patterns are basically opposite. As stated earlier, previous observational studies have focused on the AMO using SST data (e.g., Delworth and Mann 2000; Enfield et al. 2001; Gray et al. 2004; Wang et al. 2008a). Our Fig. 9a shows that the AMO signal can reach deeper than just SST manifestation: its positive (negative)

phase is associated with a warm (cool) upper ocean in the subpolar North Atlantic. Along the U.S. east coast and the Gulf Stream region, the ocean is cool (warm), as the AMO is in its positive (negative) phase. (Lozier et al. (2008) showed a warm heat content change in the tropical/subtropical Atlantic and a cool heat content change in the subpolar Atlantic between the periods of 1980-2000 and 1950-1970. However, this does not represent the warming and cooling of the AMO since these time periods do not match the positive or negative phases of the AMO.) Corresponding with the positive (negative) phase of the AMO, the upper ocean of the subtropical and subpolar North Atlantic becomes saltier (fresher), except in the Gulf Stream region where the upper ocean is fresher (saltier) (Fig. 9b). The differences in temperature and salinity between the Gulf Stream region and other North Atlantic regions suggest that the AMO is not a dominant factor in controlling oceanic temperature and salinity variations in the Gulf Stream region.

Previous studies have shown that when the AMO is in its positive (negative) phase, SSTs in the tropical North Atlantic and Caribbean Sea also become warmer (cooler) (e.g., Delworth and Mann 2000; Enfield et al. 2001; Gray et al. 2004; Wang et al. 2008a). However, our Fig. 9a shows that the upper ocean averaged over depths of 0-700 m in the western tropical North Atlantic and Caribbean Sea is cool (warm) when the AMO is in its positive (negative) phase. To investigate why this happens, we plot the zonally-averaged temperature and salinity anomaly difference between the positive and negative AMO phases (Fig. 10). Figure 10a shows that the sea surface and subsurface temperature anomalies in the tropical region of 5-25°N are out of phase; that is, the surface warming is accompanied by the subsurface cooling. Since the subsurface cooling effect is larger than the surface warming, the average temperature over depths of 0-700 m is cool, as shown in Fig. 9a. The subsurface temperature cooling in the tropical region associated with the AMO may result from the AMOC-induced variation through basin-

scale thermocline adjustment by coastal/equatorial Kelvin and Rossby wave propagations (Zhang 2007). However, the salinity anomalies do not seem to show an out-of-phase relationship between the sea surface and subsurface in the tropical region (Fig. 10b). The positive (negative) phase of the AMO is accompanied by a fresh (salty) upper ocean layer in the tropical North Atlantic and equatorial Atlantic (Fig. 10b).

As discussed earlier, the warmer and/or fresher (cooler and/or saltier) the seawater, the lighter (denser) its density. Associated with the AMO, the temperature anomalies in the upper ocean of the North Atlantic are the same sign as the salinity anomalies (Fig. 9); that is, the warming (cooling) is accompanied by an increased (decreased) level of salinity. This distribution of temperature and salinity anomaly patterns results in an opposite contribution to the potential density anomalies by the temperature and salinity changes, as shown in Figs. 11b and 11c. It is the competition between the temperature and salinity effects that determine the distribution of the potential density anomalies. On average, the resulting potential density anomalies are positive in the western part of the North Atlantic and negative in the eastern part of the subtropical and subpolar North Atlantic (Fig. 11a).

The zonally-averaged potential density anomaly difference between the eight years of positive and negative AMO phases and its contributions by temperature and salinity changes are shown in Fig. 12. Overall, the sea surface of the North Atlantic is lighter, and the subsurface becomes denser. The lighter surface water is mainly due to the surface warming associated with the AMO (Figs. 10a and 12b). The denser subsurface in the tropical North Atlantic results from the subsurface cooling effect (Figs. 10a and 12b), whereas the denser subsurface at higher latitudes is mainly due to the increase in salinity (Figs. 10b and 12c).

## 6. Meridional density gradient and the AMOC

Sections 4 and 5 show that the upper ocean of the North Atlantic displays both the long-term trend and multidecadal variations and that its variability can be divided into two regions: the subpolar and subtropical North Atlantic Ocean. A time series of temperature, salinity and potential density anomalies in the subpolar and subtropical North Atlantic Ocean averaged over depths of 0-700 m is shown in Fig. 13. As discussed earlier, the dominant variations in the temperature and salinity anomalies of the subtropical and subpolar North Atlantic Ocean are the long-term trends and the AMO signal. A close examination of Figs. 13a and 13b shows the switch time from the AMO cool to warm phases (i.e., the temperature and salinity curves cross the zero line) for the subtropical North Atlantic occurs about 8-9 years earlier than that for the subpolar North Atlantic. This seems to indicate that the temperature and salinity anomalies in the subpolar North Atlantic lag those in the subtropical North Atlantic by about 8-9 years, suggesting that the anomaly signal at the higher latitudes originates from a lower latitude through oceanic advection. This new finding provides an observational evidence for previous numerical model studies that contend that the northward advection of salinity and temperature anomalies influences on AMOC's variability (Latif et al. 2000; Thorpe et al. 2001; Vellinga and Wu 2004; Yin et al. 2006; Krebs and Timmermann 2007).

Warmer (cooler) ocean temperature decreases (increases) potential density, whereas higher (lower) level of salinity enhances (reduces) potential density. The competition between temperature and salinity fluctuations causes the potential density anomalies to differ from the AMO, although both the temperature and salinity anomalies vary with the AMO. Figures 13c and 13e also show that the potential density anomalies in the subtropical North Atlantic are dominated by temperature anomaly contribution, indicating that the density of seawater is less

influenced by salinity when the temperature is warm.

In some cases, the potential density anomalies in the subpolar North Atlantic Ocean tend to vary out of phase with those in the subtropical North Atlantic Ocean (Fig. 13c). That is, when the upper ocean density is increased (decreased) in the subpolar North Atlantic, the density is approximately decreased (increased) in the subtropical North Atlantic. Regardless of whether the out-of-phase relationship occurs, a meridional density gradient between the subpolar and subtropical North Atlantic Ocean can be formed (Fig. 13f). The meridional density gradient over the past five decades displays an upward trend with larger positive values since the 1990s. The upward trend exceeds the 99% significance level.

Theories and numerical models have been used to suggest that the strength of the meridional overturning circulation is proportional to the north-south pressure or density contrast between the Northern and Southern Hemispheres (e.g., Stommel 1961; Bryan and Cox 1967; Hughes and Weaver 1994; Park 1999; Scott et al. 1999; Thorpe et al. 2001; Kuhlbrodt et al. 2007). Based on the observed patterns presented here, we hypothesize that the strength of the AMOC is related to the meridional density gradient between the subpolar and subtropical North Atlantic Ocean. To test this hypothesis, we used oceanic reanalysis products to calculate the streamfunction of the AMOC as shown by Eq. (2). Figure 14 shows the mean streamfunction from the SODA, GECCO, and GFDL ocean reanalysis products. Although each product displays different distributions and amplitudes of streamfunction, they all show a large-scale flow of the AMOC which is represented by a clockwise circulation cell consisting of an upper layer northward flow, a sinking flow in the northern high latitudes, and a southward return flow at depth.

The maximum streamfunction at 30°N is chosen to represent the AMOC's strength. The

time series of the AMOC's strength from three products are shown in Fig. 15. Over the past decades the AMOC has not slowed down in all of three products; rather, they all show upward trends. The result is opposite to that of Bryden et al. (2005) who claimed that the AMOC has been slowed down. The linear upward trends in Fig. 15 are all statistically significant at the 95% level. The upward trend rate for the ensemble average of three products is 0.0039 Sv/month or 0.47 Sv/decade (1 Sv= $10^6$  m<sup>3</sup>/s). That is, the AMOC has been secularly strengthened since 1950 at an increased rate of about 0.5 Sv for every decade. However, we should keep in mind that whether or not the AMOC shows an upward trend may depend on the time period of oceanic reanalysis products (e.g., Rabe et al. 2008) and oceanic reanalysis products used (e.g., Balmaseda et al. 2007).

To examine the relationship between the AMOC and meridional density gradient, we use the SODA reanalysis from 1974 to 2005 (we skip the model data before 1974 since they show unexpected variations of the AMOC and observations are more after the 1970s) which assimilate available temperature and salinity observations. Consistent with the observed result shown in Fig. 13f, the meridional density gradient between the subpolar and subtropical North Atlantic from the SODA product also displays an upward trend with larger positive values in the 1990s (not shown). Figure 16 shows the scatter plot of the AMOC's strength versus the meridional density gradient between the subpolar and subtropical North Atlantic Ocean. The AMOC's strength is strongly related to the meridional density gradient between the subpolar and subtropical North Atlantic Ocean, with a correlation coefficient of 0.52 (above the 99% significance level). If the SODA time series are extended back to 1958, the correlation is still significant in spite of with a correlation reduction. This indicates that the meridional density gradient may be a driving force for the AMOC in the SODA reanalysis product, consistent with

the observed features reported in this paper.

## **7. Summary and discussion**

The paper uses observational data over the past five decades to analyze variability of temperature, salinity and density in the upper ocean of the North Atlantic. The analyses of these observations, along with oceanic reanalysis products, provide some insights on the Atlantic meridional overturning circulation (AMOC). The major results and findings of the present paper can be summarized as follows:

- For the long-term trend, the upper ocean of the subpolar North Atlantic is becoming cooler and fresher, whereas the subtropical North Atlantic is becoming warmer and saltier. Owing to opposite contributions by temperature and salinity trends, the density trend in the subpolar North Atlantic is small and the density in the subtropical North Atlantic is secularly decreased.
- On a multidecadal timescale, both the temperature and salinity anomalies in the upper ocean of the North Atlantic show the AMO signal with a warmer and saltier ocean after 1995. However, the density anomalies in the North Atlantic Ocean do not precisely coincide with the AMO because of the compensating effect of temperature and salinity on the potential density.
- These variations do not result in a density reduction in the subpolar North Atlantic for slowing down the AMOC. Indeed, the variations in the meridional density gradient between the subpolar and subtropical North Atlantic Ocean suggest that the AMOC has become stronger over the past decades. A further analysis of some oceanic reanalysis products supports these observed results.

- The temperature and salinity anomalies in the subpolar North Atlantic seem to lag those in the subtropical North Atlantic by about 8-9 years, suggesting that the anomaly signal at the higher latitudes originates from the lower latitudes through oceanic advection. This new finding provides an observational evidence for previous numerical model studies that contend that the northward advection of salinity and temperature anomalies influences on AMOC's variability

The temperature variation of the North Atlantic Ocean is very important since it can affect Atlantic hurricane activity and rainfall in North America (e.g., Goldenberg et al. 2001; Enfield et al. 2001; McCabe et al. 2004; Wang et al. 2008b). Both global warming and natural climate variability contribute to the ocean temperature variation in the North Atlantic. If global warming leads to a substantial weakening of the AMOC as proposed by Manabe et al. (1991) and others, the weakening of the AMOC will be associated with a cooling in the North Atlantic Ocean, which will compensate partly for the greenhouse warming in the North Atlantic Ocean. At the same time, the oscillation of the AMO can either warm or cool the North Atlantic Ocean dependent on its phases. Here we observe that the upper ocean of the subpolar North Atlantic is secularly becoming cooler over the past five decades and has been warmer since 1995 in association with the positive phase of the AMO. Obviously, they compete each other for the warming (or cooling) in the North Atlantic Ocean. The mechanisms of ocean temperature (also salinity and density) variations in the North Atlantic need to be further studied.

The relationship of the AMOC with seawater property in the North Atlantic is worthy discussing. For the long-term trend, the upper ocean of the subpolar North Atlantic is observed to become cooler and fresher, whereas the AMOC has been secularly strengthened. This seems to be inconsistent with the notion that as the AMOC is enhanced (reduced), an increase

(decrease) in heat and salinity occurs in the subpolar ocean owing to the increasing (decreasing) northward transport of heat and salt from the subtropical ocean. In fact, observations presented in this paper suggest that the meridional density gradient between the subpolar and subtropical North Atlantic Ocean determines the AMOC's strength for the long-term trend. Although the cooling and freshening are observed in the subpolar North Atlantic Ocean, the density gradient between the subpolar and subtropical North Atlantic Ocean is increased. This explains why an increase of the AMOC can be associated with a cooler and fresher subpolar North Atlantic Ocean.

The yearly temperature data used in this study are only to a depth of 700 m, as our analyses are focused on the upper ocean of the North Atlantic. Further studies of the deeper ocean using numerical models and observations are needed to investigate the observed features and mechanisms reported here. The results presented in this study have at least two implications. First, a protocol for measuring the meridional density gradient between the subpolar and subtropical North Atlantic Ocean may be useful for monitoring AMOC variability. Secondly, how/whether the AMOC is weakened under future global warming will be probably dependent upon the density variation patterns occurring in the North Atlantic basin, determined by the combined fluctuations of both oceanic temperature and salinity.

**Acknowledgments.** We thank reviewers' suggestions and comments on this manuscript. We also thank Tim Boyer who provided us the updated salinity data before its public release. Gail Derr gave some editorial comments on an early version of the manuscript. This work was supported by a grant from National Oceanic and Atmospheric Administration (NOAA) Climate Program Office and by the base funding of NOAA Atlantic Oceanographic and Meteorological

Laboratory (AOML). The findings and conclusions in this report are those of the author(s) and do not necessarily represent the views of the funding agency.

## References

- Balmaseda MA, Smith GC, Haines K, Anderson D, Palmer TN, Vidard A (2007) Historical reconstruction of the Atlantic meridional overturning circulation from the ECMWF operational ocean reanalysis. *Geophys Res Lett* 34: L23615. Doi:10.1029/2007GL031645.
- Bell GD, Chelliah M (2006) Leading tropical modes associated with interannual and multidecadal fluctuations in north Atlantic hurricane activity. *J Clim* 19: 590-612.
- Boyer TP, Levitus S, Antonov JI, Locarnini RA, Garcia HE (2005) Linear trends in salinity for the World Ocean, 1955-1998. *Geophys Res Lett* 32: L01604. doi:10.1029/2004GL021791
- Boyer TP, Coauthors (2006) World Ocean Database 2005, NOAA Atlas NESDIS, vol. 60, edited by S. Levitus, 190 pp., U.S. Gov. Print. Off., Washington D. C.
- Boyer TP, Coauthors (2007) Changes in freshwater content in the North Atlantic Ocean 1955-2006. *Geophys Res Lett* 34: L16603. doi:10.1029/2007GL030126.
- Bryan K, Cox M (1967) A numerical investigation of the oceanic general circulation. *Tellus* 19: 54-80.
- Bryden HL, Longworth HL, Cunningham (2005) Slowing of the Atlantic meridional overturning circulation at 25°N. *Nature* 438: 655-657.
- Carton JA, Giese BS (2008) A reanalysis of ocean climate using Simple Ocean Data Assimilation (SODA). *Mon Wea Rev* 136: 2999-3017.
- Conkright ME, Coauthors (2002) World Ocean Database 2001, vol. 1, NOAA Atlas NESDIS 42, edited by S. Levitus, 167 pp., U.S. Gov. Print. Off., Washington D. C.
- Curry R, Dickson B, Yashayaev I (2003) A change in the freshwater balance of the Atlantic Ocean over the past four decades. *Nature* 426: 826-829.

- Delworth TL, Mann ME (2000) Observed and simulated multidecadal variability in the Northern Hemisphere. *Clim Dyn* 16: 661-676.
- Dickson B, Coauthors (2002) Rapid freshening of the deep North Atlantic Ocean over the past four decades. *Nature* 416: 832-837.
- Dijkstra HA, te Raa L, Schmeits M, Gerrits J (2006) On the physics of the Atlantic multidecadal oscillation. *Ocean Dyn* 56: 36-50.
- Dong BW, Sutton TT (2002) Adjustment of the coupled ocean-atmosphere system to a sudden change in the thermohaline circulation. *Geophys Res Lett* 29: 1728. doi: 10.1029/2002GL015229
- Enfield DB, Mestas-Nunez AM, Trimble PJ (2001) The Atlantic Multidecadal Oscillation and its relationship to rainfall and river flows in the continental US. *Geophys Res Lett* 28: 2077-2080.
- Gill AE (1982) *Atmosphere-Ocean Dynamics*. Academic Press, New York, 662 pp.
- Goldenberg SB, Landsea CW, Maestas-Nunez AM, Gray WM (2001) The recent increase in Atlantic hurricane activity: Causes and implications. *Science* 293: 474-479.
- Gray ST, Graumlich JL, Betancourt JL, Pederson GT (2004) A tree-ring based reconstruction of the Atlantic Multidecadal Oscillation since 1567 A.D. *Geophys Res Lett* 31: L12205. doi:10.1029/2004GL019932.
- Hegerl GC, Coauthors (2007) Understanding and Attributing Climate Change. In: *Climate Change 2007: The Physical Science Basis. Contribution of Working Group I to the Fourth Assessment Report of the Intergovernmental Panel on Climate Change*, edited by S. Solomon et al., Cambridge University Press, Cambridge, United Kingdom and New York, NY, USA.

- Huang B, Shukla J (2005) The ocean-atmospheric interactions in the tropical and subtropical Atlantic Ocean. *J Clim* 18: 1652-1672.
- Hughes T, Weaver A (1994) Multiple equilibrium of an asymmetric two-basin model. *J Phys Oceanogr* 24: 619-637.
- Josey SA, Kent EC, Taylor PK (1998) The Southampton Oceanography Centre (SOC) Ocean-Atmosphere Heat, Momentum and Freshwater Flux Atlas. *Southampton Oceanography Centre Report No. 6*, 30 pp.
- Knight JR, Allan RJ, Folland CK, Vellinga M, Mann ME (2005) A signature of persistent natural thermohaline circulation cycles in observed climate. *Geophys Res Lett* 32: L20708.  
doi:10.1029/2005GL024233
- Kohl A., Dommenges D, Ueyoshi K, Stammer D (2006) The Global ECCO 1952 to 2001 ocean synthesis. ECCO Report No. 40.
- Krebs U, Timmermann A (2007) Tropical air-sea interactions accelerate the recovery of the Atlantic Meridional Overturning Circulation after a major shutdown. *J Clim* 20: 4940–4956.
- Kuhlbrodt T, Coauthors (2007) On the driving processes of the Atlantic meridional overturning circulation. *Rev Geophys* 45: RG2001. doi:10.1029/2004RG000166
- Latif M, Roeckner E, Mikolajewicz U, Voss R (2000) Tropical stabilization of the thermohaline circulation in a greenhouse warming simulation. *J Clim* 13: 1809-1813.
- Lozier MS, Leadbetter S, Williams RG, Roussenov V, Reed MSC, Moore NJ (2008) The spatial pattern and mechanisms of heat-content change in the North Atlantic. *Science* 319: 800-803.
- Manabe S, Stouffer RJ, Spelman MJ, Bryan K (1991) Transient response of a coupled ocean-atmosphere model to gradual changes of atmospheric CO<sub>2</sub>. Part I: Annual mean response. *J. Clim* 4: 785-818.

- Mann ME, Emanuel KA (2006) Atlantic hurricane trends linked to climate change. *Eos Trans AGU* 87: 233-244. doi:10.1029/2006EO240001
- McCabe G, Palecki M, Betancourt J (2004) Pacific and Atlantic Ocean influences on multidecadal drought frequency in the United States. *Proc Nat Acad Sci* 101: 4136-4141.
- Park YG (1999) The stability of thermohaline circulation in a two-box model. *J Phys Oceanogr* 29: 3101-3110.
- Rabe B, Schott FA, Kohl A (2008) Mean circulation and variability of the tropical Atlantic during 1952-2001 in the GECCO assimilation fields. *J Phys Oceanogr* 38: 177-192.
- Rosati A, Harrison M, Wittenberg A, Zhang S (2004) NOAA/GFDL ocean data assimilation activities. CLIVAR Workshop on Ocean Reanalysis, NCAR, Boulder, CO, 9 November 2004.
- Santer BD, Coauthors (2006) Forced and unforced ocean temperature changes in Atlantic and Pacific tropical cyclogenesis regions. *Proc Nat Acad Sci* 203: 13905-13910.
- Schmittner A, Chiang JCH, Hemming SR (2007) *Ocean circulation: Mechanisms and impacts*. Geophysical Monograph Series 173, American Geophysical Union, Washington, D. C., 392 pp.
- Scott J, Marotzke J, Stone P (1999) Interhemispheric thermohaline circulation in a coupled box model. *J Phys Oceanogr* 29: 351-365.
- Stommel H (1961) Thermohaline convection with two stable regimes of flow. *Tellus* 13: 224-230.
- Thorpe RB, Gregory JM, Johns TC, Wood RA, Mitchell JFB (2001) Mechanisms determining the Atlantic thermohaline circulation response to greenhouse gas forcing in a non-flux-adjusted coupled climate model. *J Clim* 14: 3102-3116.

- Timmermann A, Coauthors (2007) The influence of a weakening of the Atlantic meridional overturning circulation on ENSO. *J Clim* 20: 4899-4919.
- Vellinga M, Wood RA (2002) Global climatic impacts of a collapse of the Atlantic thermohaline circulation. *Clim Changes* 54: 251-267.
- Vellinga M, Wu P (2004) Low-latitude freshwater influences on centennial variability of the Atlantic thermohaline circulation. *J Clim* 17: 4498–4511.
- Wang C, Lee SK, Enfield DB (2008a) Atlantic warm pool acting as a link between Atlantic multidecadal oscillation and Atlantic tropical cyclone activity. *Geochem Geophys Geosyst* 9: Q05V03. doi:10.1029/2007GC001809
- Wang C, Lee SK, Enfield DB (2008b) Climate response to anomalously large and small Atlantic warm pools during the summer. *J Clim* 21: 2437–2450.
- Yin J, Schlesinger ME, Andronova NG, Malyshev S, Li B (2006) Is a shutdown of the thermohaline circulation irreversible? *J Geophys Res* 111: D12104.  
doi:10.1029/2005JD006562.
- Zhang D, McPhaden MJ, Johns WE (2003) Observational evidence for flow between the subtropical and tropical Atlantic: The Atlantic subtropical cells. *J Phys Oceanogr* 33: 1783-1797.
- Zhang R (2007) Anticorrelated multidecadal variations between surface and subsurface tropical North Atlantic. *Geophys Res Lett* 34: L12713. doi:10.1029/2007GL030225.
- Zhang R, Delworth TL, Held I (2007) Can the Atlantic Ocean drive the observed multidecadal variability in Northern Hemisphere mean temperature? *Geophys Res Lett* 34: L02709.  
doi:10.1029/2006GL028683.

## Figure Captions

**Figure 1.** The annual mean (a) E-P (mm/day), (b) SSS (psu), (c) SST ( $^{\circ}\text{C}$ ) and (d) surface potential density ( $\text{kg}/\text{m}^3$ ) in the North Atlantic.

**Figure 2.** The zonally-averaged (between  $80^{\circ}\text{W}$ - $20^{\circ}\text{E}$ ) annual mean (a) salinity (psu), (b) temperature ( $^{\circ}\text{C}$ ), and (c) potential density ( $\text{kg}/\text{m}^3$ ) as a function of depth and latitude.

**Figure 3.** The annual mean (a) salinity (psu), (b) temperature ( $^{\circ}\text{C}$ ) and (c) potential density ( $\text{kg}/\text{m}^3$ ) averaged over depths of 0-700 m.

**Figure 4.** The long-term linear trend patterns of the (a) temperature anomalies ( $^{\circ}\text{C}/\text{decade}$ ) and (b) salinity anomalies ( $10^{-2}$  psu/decade) averaged over depths of 0-700 m.

**Figure 5.** The long-term linear trend patterns of the potential density anomalies ( $\text{kg}/\text{m}^3$  per decade) averaged over depths of 0-700 m. Shown are the (a) total trend of the potential density anomalies, (b) potential density trend contributed by temperature trend and (c) potential density trend contributed by salinity trend.

**Figure 6.** The zonally-averaged (between  $80^{\circ}\text{W}$ - $20^{\circ}\text{E}$ ) long-term linear trends of the (a) temperature ( $^{\circ}\text{C}/\text{decade}$ ) and (b) salinity anomalies ( $10^{-2}$  psu/decade) as a function of depth and latitude.

**Figure 7.** The zonally-averaged (between 80°W-20°E) long-term linear trends of the potential density anomalies ( $\text{kg/m}^3$  per decade) as a function of depth and latitude. Shown are the (a) total linear trend of potential density anomalies, (b) potential density trend contributed by temperature trend and (c) potential density trend contributed by salinity trend.

**Figure 8.** The time series of the detrended temperature ( $^{\circ}\text{C}$ ), salinity (psu) and potential density ( $\text{kg/m}^3$ ) anomalies in the subpolar North Atlantic Ocean of 50°N-75°N, 60°W-10°E averaged over depths of 0-700 m. Shown are the (a) temperature (red) and salinity (green) anomalies, (b) potential density anomalies, and (c) potential density anomalies contributed by temperature (red) and salinity (green) anomalies.

**Figure 9.** The detrended (a) temperature ( $^{\circ}\text{C}$ ) and (b) salinity (psu) anomaly difference between the positive and negative AMO phases. The positive AMO phase is represented by the eight-year period of 1996-2003 and the negative phase is by the eight-year period of 1976-1983. Shown are the upper ocean anomalies averaged over depths of 0-700 m.

**Figure 10.** The zonally-averaged detrended (a) temperature ( $^{\circ}\text{C}$ ) and (b) salinity (psu) anomaly difference between the positive and negative AMO phases as a function of depth and latitude. The positive AMO phase is represented by the eight-year period of 1996-2003 and the negative phase is by the eight-year period of 1976-1983. The zonal average is from 80°W-20°E.

**Figure 11.** The detrended potential density anomaly ( $\text{kg/m}^3$ ) difference between the positive and negative AMO phases. Shown are the (a) detrended potential density anomalies, (b) potential

density anomalies contributed by temperature anomalies and (c) potential density anomalies contributed by salinity anomalies. The positive AMO phase is represented by the eight-year period of 1996-2003 and the negative phase is by the eight-year period of 1976-1983. Shown are the upper ocean anomalies averaged over depths of 0-700 m.

**Figure 12.** The zonally-averaged detrended potential density anomaly ( $\text{kg/m}^3$ ) difference between the positive and negative AMO phases as a function of depth and latitude. Shown are the (a) detrended potential density anomalies, (b) potential density anomalies contributed by temperature anomalies and (c) potential density anomalies contributed by salinity anomalies. The positive AMO phase is represented by the eight-year period of 1996-2003 and the negative phase is by the eight-year period of 1976-1983. The zonal average is from  $80^\circ\text{W}$ - $20^\circ\text{E}$ .

**Figure 13.** The time series of the temperature ( $^\circ\text{C}$ ), salinity (psu) and potential density ( $\text{kg/m}^3$ ) anomalies in the upper ocean (0-700 m) of the North Atlantic. Shown are (a) the temperature anomalies in the subtropical (red) and subpolar (green) North Atlantic, (b) the salinity anomalies in the subtropical (red) and subpolar (green) North Atlantic, (c) the potential density anomalies in the subtropical (red) and subpolar (green) North Atlantic, (d) the potential density anomalies contributed by temperature (red) and salinity (green) in the subpolar North Atlantic, (e) the potential density anomalies contributed by temperature (red) and salinity (green) in the subtropical North Atlantic, and (f) the meridional potential density gradient between the subpolar and subtropical North Atlantic. The straight line in (f) is the linear trend which exceeds the 99% significance level. The subpolar and subtropical North Atlantic are defined in the regions of  $50^\circ\text{N}$ - $75^\circ\text{N}$ ,  $60^\circ\text{W}$ - $10^\circ\text{E}$  and  $25^\circ\text{N}$ - $50^\circ\text{N}$ ,  $60^\circ\text{W}$ - $10^\circ\text{E}$ , respectively.

**Figure 14.** The mean streamfunction ( $S_v$ ) calculated from the (a) SODA, (b) GECCO, and (c) GFDL ocean reanalysis products. The AMOC is represented by a clockwise circulation cell consisting of an upper layer northward flow, a sinking flow in the northern high latitudes and a southward return flow at depth.

**Figure 15.** The time series of the maximum streamfunction ( $S_v$ ) at  $30^\circ\text{N}$  from the SODA, GECCO, and GFDL ocean reanalysis products. The black curve is the ensemble average of three products. The straight lines are the linear trends that are fitted to their respective time series. An 11-month running mean is applied to the indices.

**Figure 16.** The scatter plot of the AMOC strength ( $S_v$ ;  $1 S_v = 10^6 \text{ m}^3/\text{s}$ ) versus the meridional potential density gradient ( $\text{kg}/\text{m}^3$ ) between the subpolar and subtropical North Atlantic Ocean, calculated from the SODA reanalysis from 1974-2005. The AMOC strength is measured by the maximum streamfunction at  $30^\circ\text{N}$ . The meridional potential density gradient is computed by the potential density anomaly (after removing seasonal cycle) difference between the regions of  $60^\circ\text{W}-10^\circ\text{W}$ ,  $52^\circ\text{N}-75^\circ\text{N}$  and  $70^\circ\text{W}-10^\circ\text{W}$ ,  $25^\circ\text{N}-50^\circ\text{N}$ . An 11-month running mean is applied to both indices before the scatter plot. The straight line represents the linear regression.

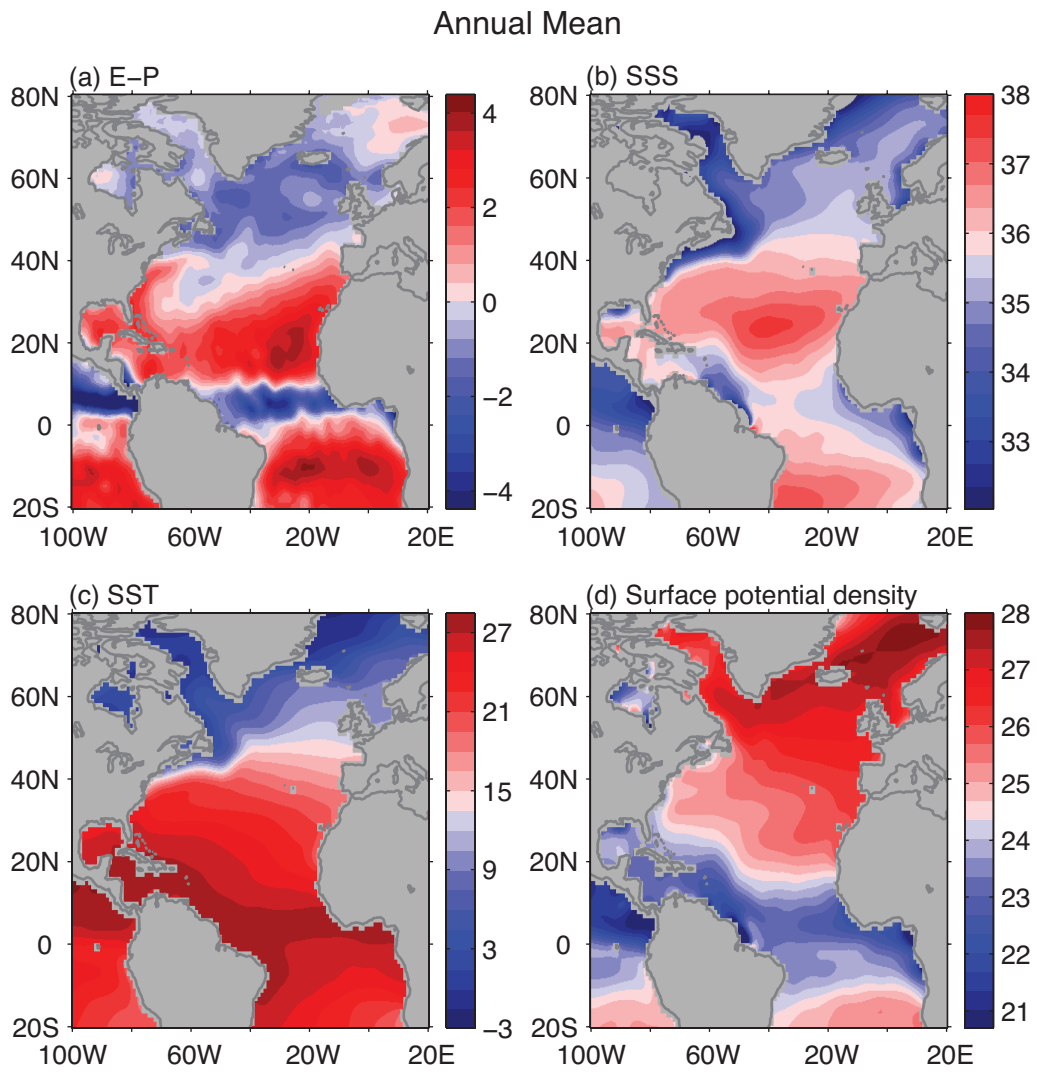


**Figure 1.** The annual mean (a) E-P (mm/day), (b) SSS (psu), (c) SST ( $^{\circ}$ C) and (d) surface potential density ( $\text{kg/m}^3$ ) in the North Atlantic.

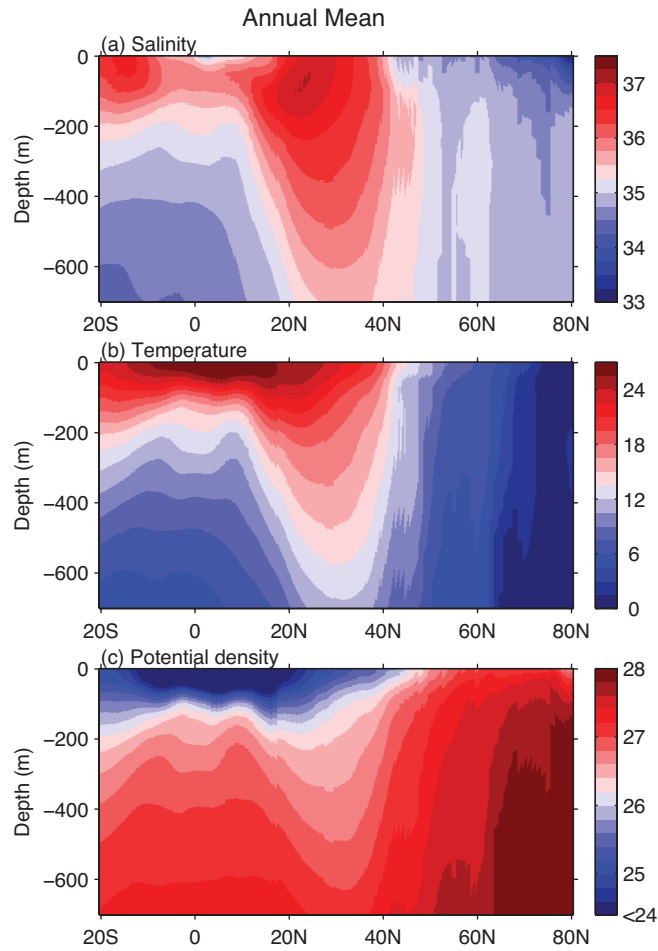


**Figure 2.** The zonally-averaged (between 80°W-20°E) annual mean (a) salinity (psu), (b) temperature (°C), and (c) potential density ( $\text{kg}/\text{m}^3$ ) as a function of depth and latitude.

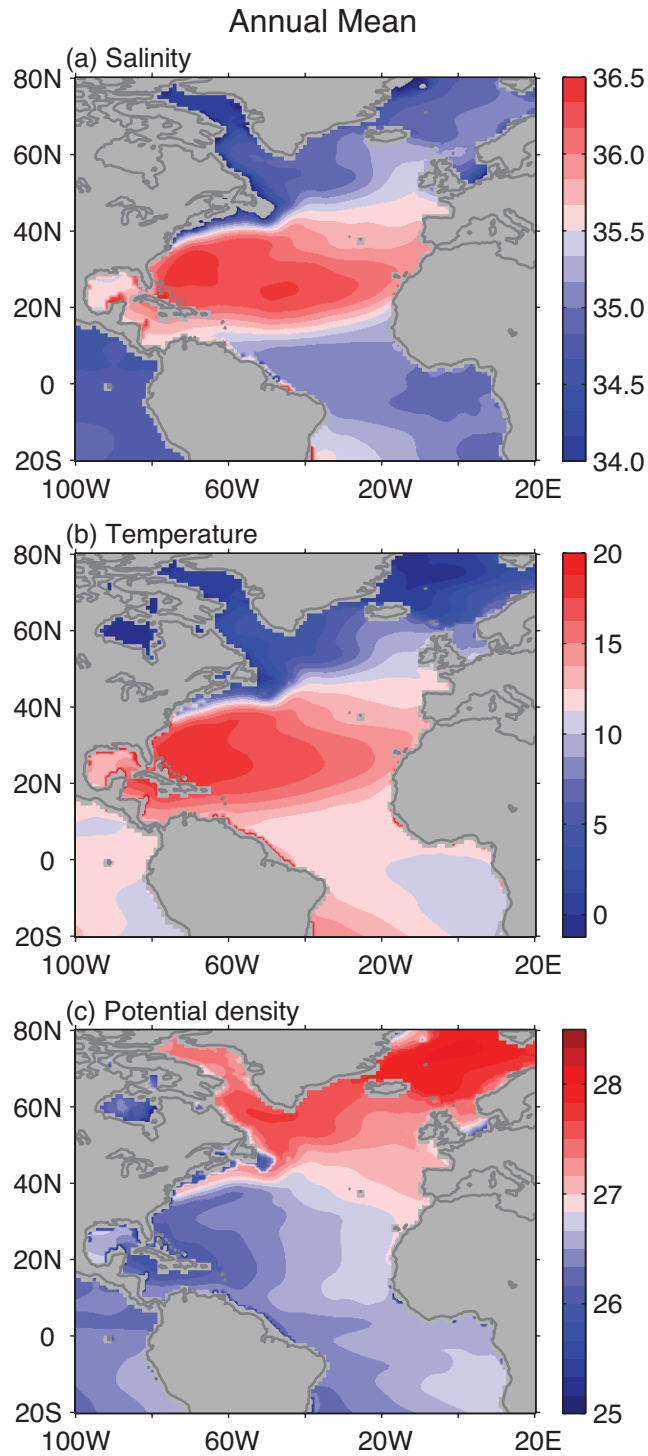


**Figure 3.** The annual mean (a) salinity (psu), (b) temperature ( $^{\circ}\text{C}$ ) and (c) potential density ( $\text{kg}/\text{m}^3$ ) averaged over depths of 0-700 m.

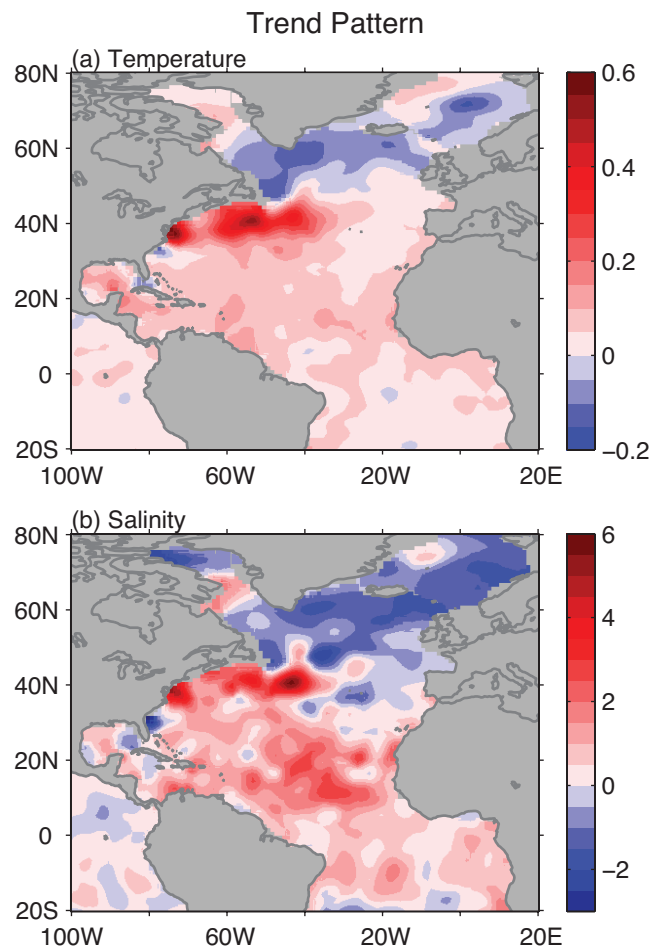


**Figure 4.** The long-term linear trend patterns of the (a) temperature anomalies ( $^{\circ}\text{C}/\text{decade}$ ) and (b) salinity anomalies ( $10^{-2}$  psu/decade) averaged over depths of 0-700 m.

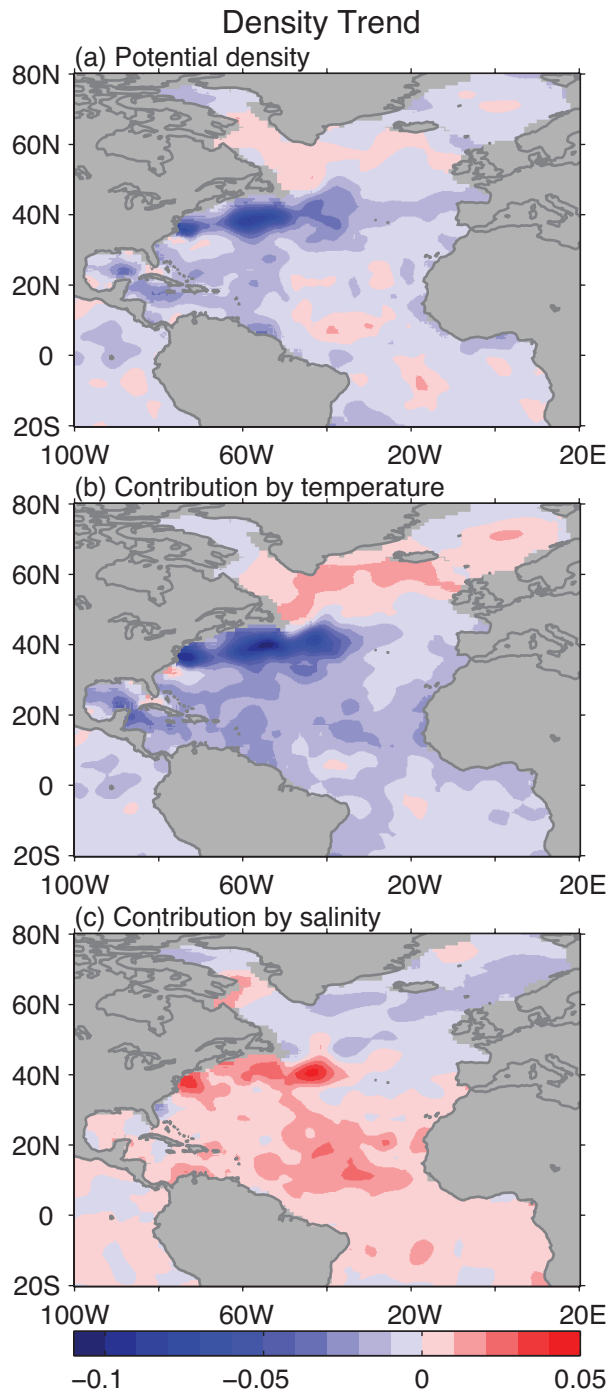


**Figure 5.** The long-term linear trend patterns of the potential density anomalies ( $\text{kg/m}^3$  per decade) averaged over depths of 0-700 m. Shown are the (a) total trend of the potential density anomalies, (b) potential density trend contributed by temperature trend and (c) potential density trend contributed by salinity trend.

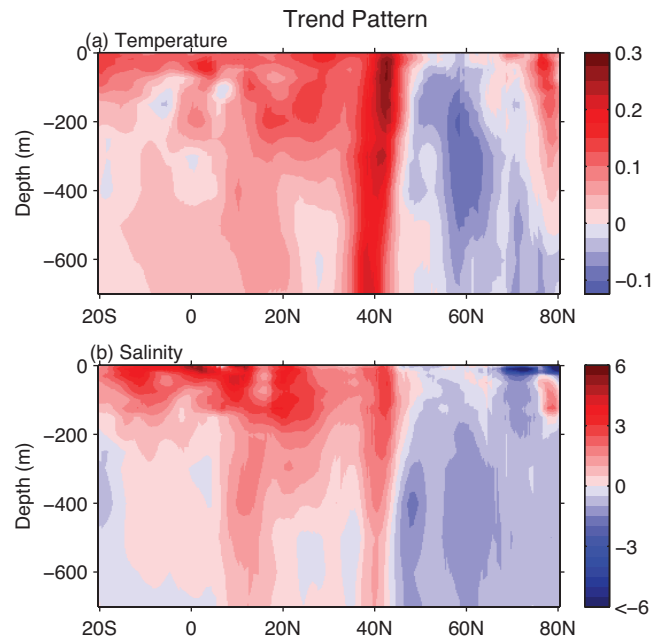


**Figure 6.** The zonally-averaged (between 80°W-20°E) long-term linear trends of the (a) temperature (°C/decade) and (b) salinity anomalies ( $10^{-2}$  psu/decade) as a function of depth and latitude.

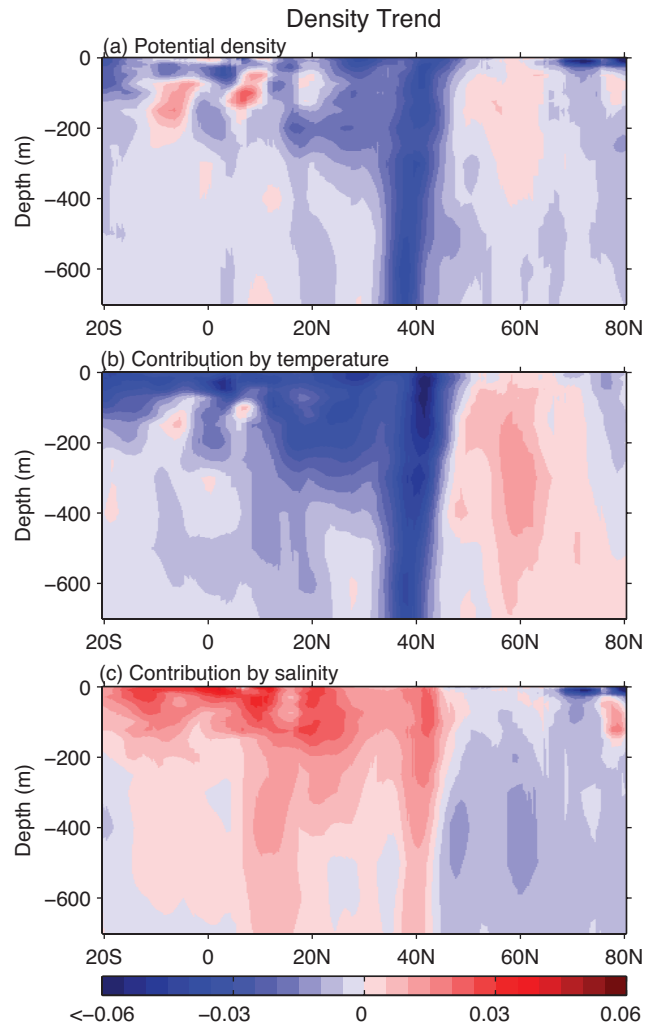


**Figure 7.** The zonally-averaged (between 80°W-20°E) long-term linear trends of the potential density anomalies ( $\text{kg/m}^3$  per decade) as a function of depth and latitude. Shown are the (a) total linear trend of potential density anomalies, (b) potential density trend contributed by temperature trend and (c) potential density trend contributed by salinity trend.

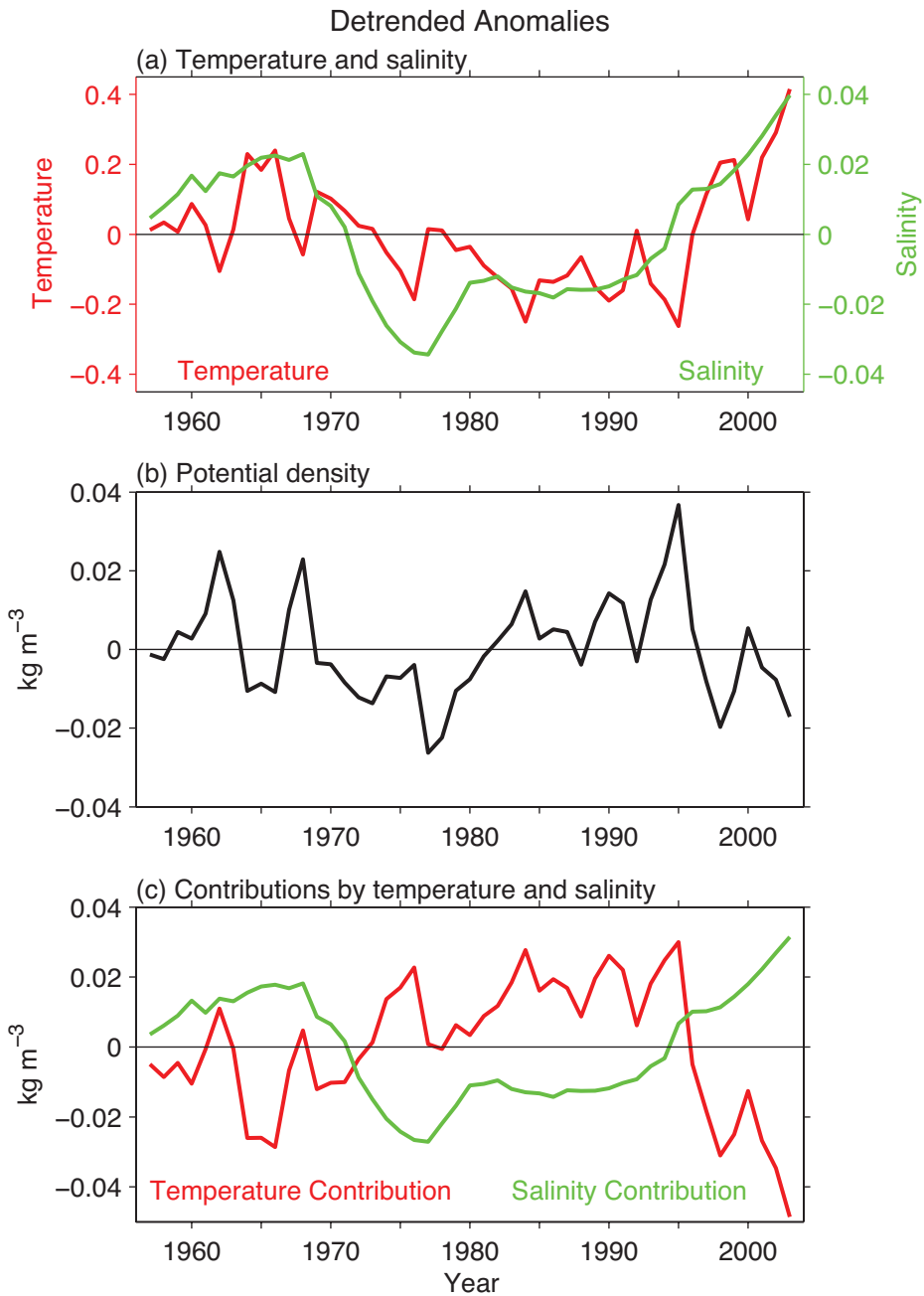


**Figure 8.** The time series of the detrended temperature ( $^{\circ}\text{C}$ ), salinity (psu) and potential density ( $\text{kg}/\text{m}^3$ ) anomalies in the subpolar North Atlantic Ocean of  $50^{\circ}\text{N}$ - $75^{\circ}\text{N}$ ,  $60^{\circ}\text{W}$ - $10^{\circ}\text{E}$  averaged over depths of 0-700 m. Shown are the (a) temperature (red) and salinity (green) anomalies, (b) potential density anomalies, and (c) potential density anomalies contributed by temperature (red) and salinity (green) anomalies.

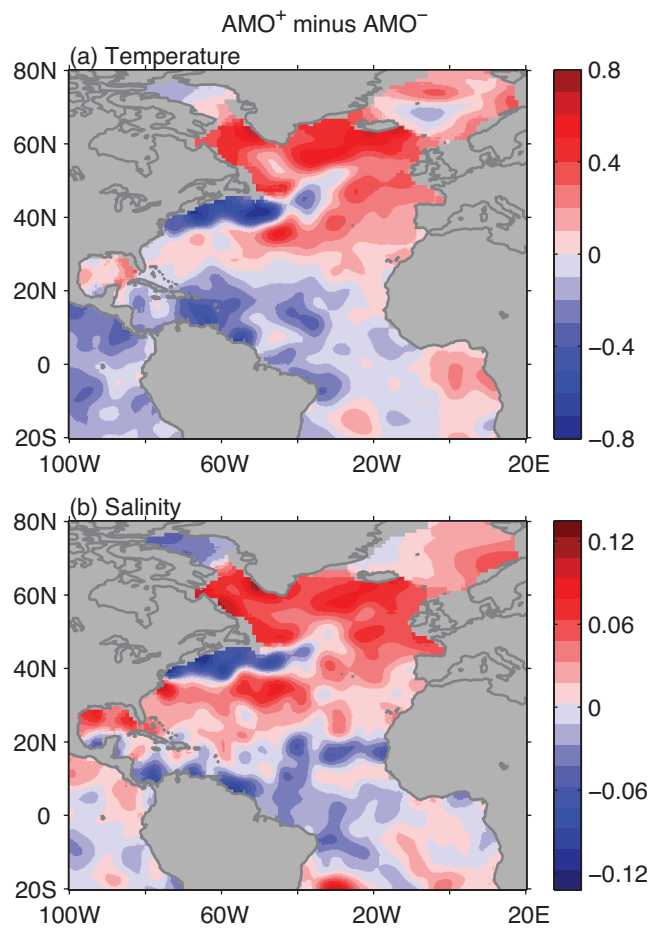


**Figure 9.** The detrended (a) temperature (°C) and (b) salinity (psu) anomaly difference between the positive and negative AMO phases. The positive AMO phase is represented by the eight-year period of 1996-2003 and the negative phase is by the eight-year period of 1976-1983. Shown are the upper ocean anomalies averaged over depths of 0-700 m.

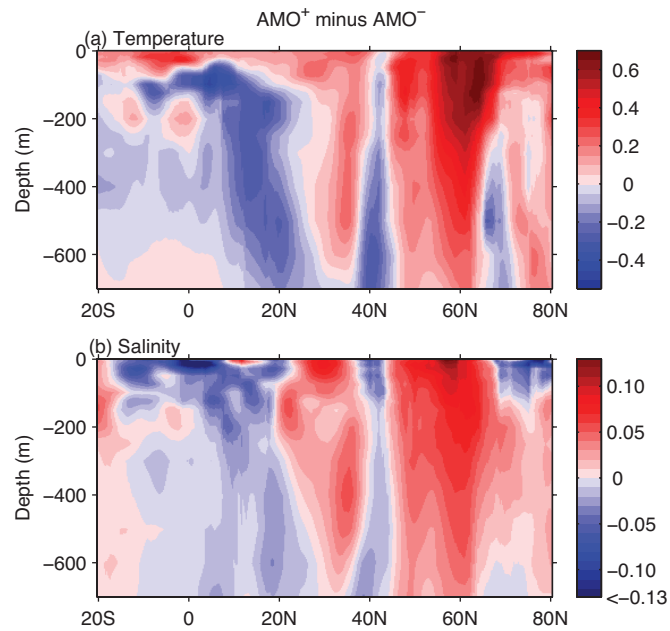


**Figure 10.** The zonally-averaged detrended (a) temperature ( $^{\circ}\text{C}$ ) and (b) salinity (psu) anomaly difference between the positive and negative AMO phases as a function of depth and latitude. The positive AMO phase is represented by the eight-year period of 1996-2003 and the negative phase is by the eight-year period of 1976-1983. The zonal average is from  $80^{\circ}\text{W}$ - $20^{\circ}\text{E}$ .

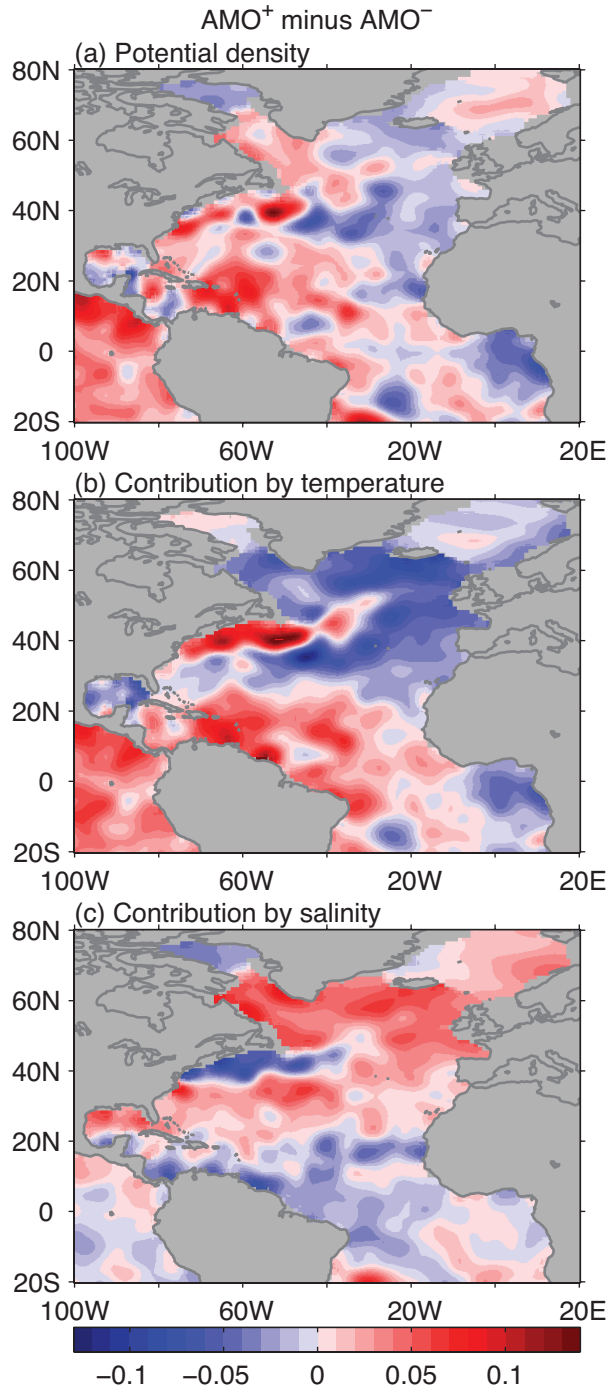


**Figure 11.** The detrended potential density anomaly ( $\text{kg/m}^3$ ) difference between the positive and negative AMO phases. Shown are the (a) detrended potential density anomalies, (b) potential density anomalies contributed by temperature anomalies and (c) potential density anomalies contributed by salinity anomalies. The positive AMO phase is represented by the eight-year period of 1996-2003 and the negative phase is by the eight-year period of 1976-1983. Shown are the upper ocean anomalies averaged over depths of 0-700 m.

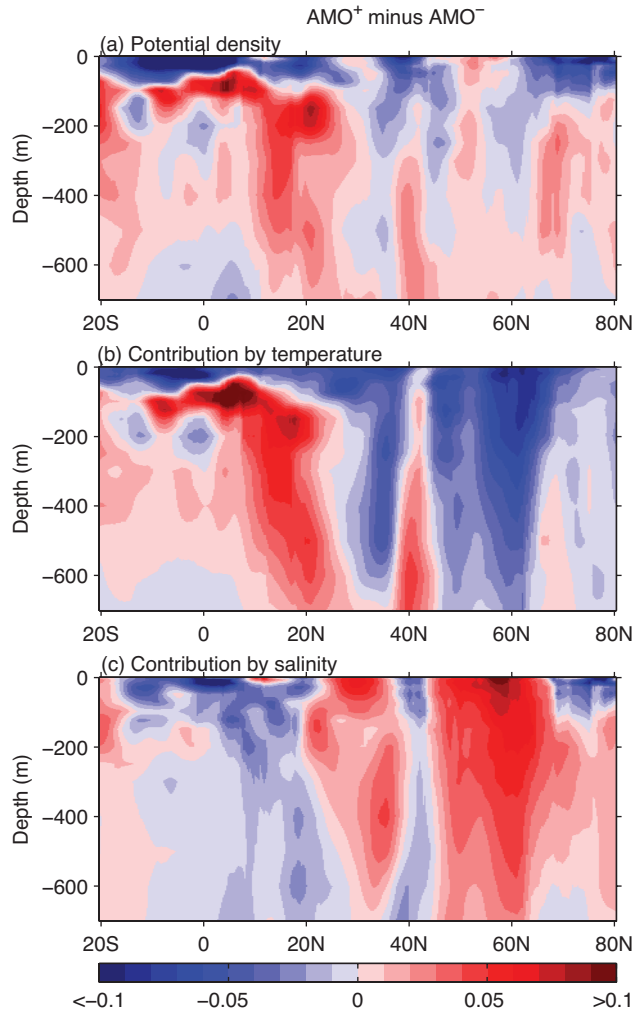


**Figure 12.** The zonally-averaged detrended potential density anomaly ( $\text{kg/m}^3$ ) difference between the positive and negative AMO phases as a function of depth and latitude. Shown are the (a) detrended potential density anomalies, (b) potential density anomalies contributed by temperature anomalies and (c) potential density anomalies contributed by salinity anomalies. The positive AMO phase is represented by the eight-year period of 1996-2003 and the negative phase is by the eight-year period of 1976-1983. The zonal average is from  $80^\circ\text{W}$ - $20^\circ\text{E}$ .

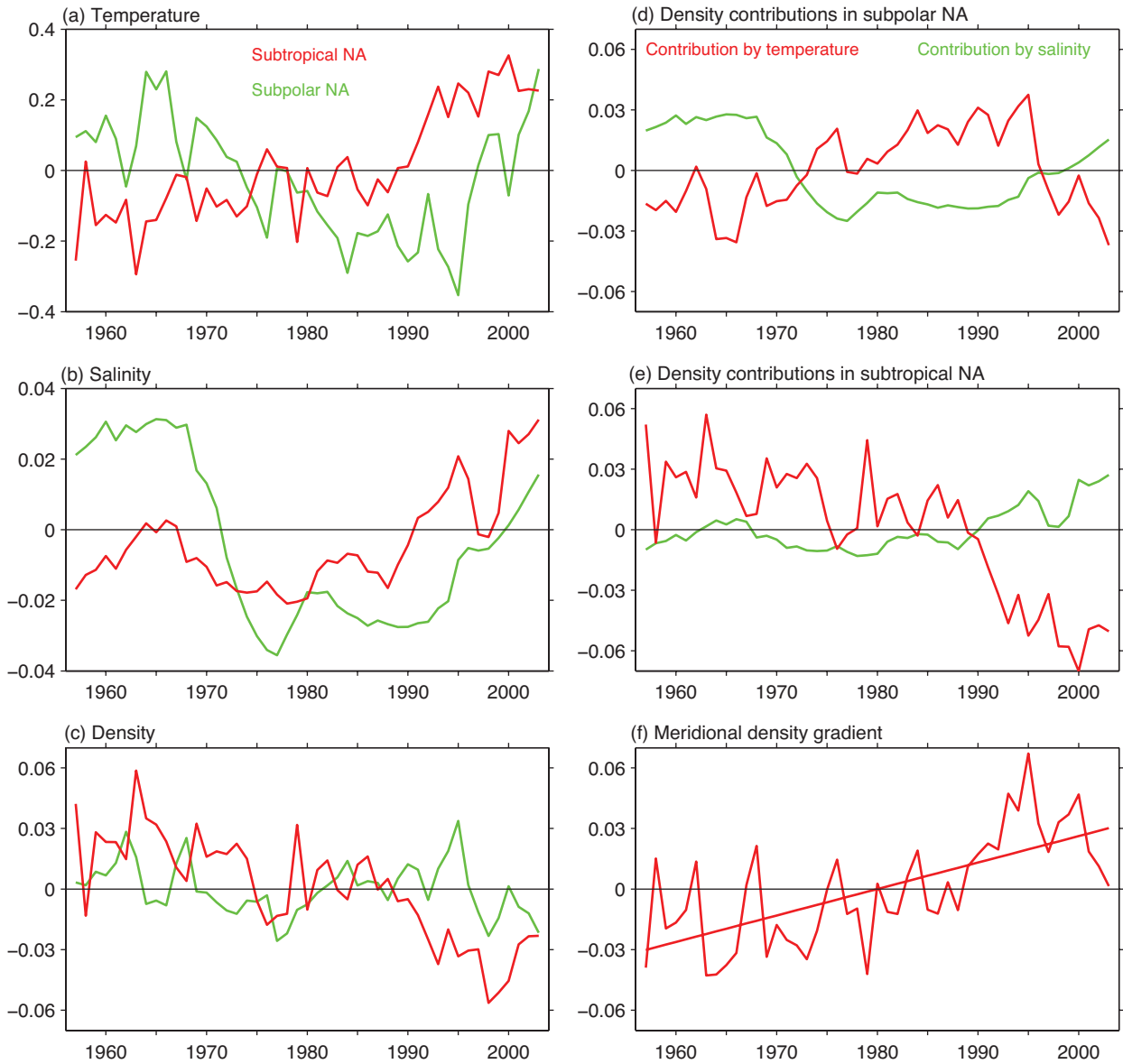


**Figure 13.** The time series of the temperature ( $^{\circ}\text{C}$ ), salinity (psu) and potential density ( $\text{kg/m}^3$ ) anomalies in the upper ocean (0-700 m) of the North Atlantic. Shown are (a) the temperature anomalies in the subtropical (red) and subpolar (green) North Atlantic, (b) the salinity anomalies in the subtropical (red) and subpolar (green) North Atlantic, (c) the potential density anomalies in the subtropical (red) and subpolar (green) North Atlantic, (d) the potential density anomalies contributed by temperature (red) and salinity (green) in the subpolar North Atlantic, (e) the potential density anomalies contributed by temperature (red) and salinity (green) in the subtropical North Atlantic, and (f) the meridional potential density gradient between the subpolar and subtropical North Atlantic. The straight line in (f) is the linear trend which exceeds the 99% significance level. The subpolar and subtropical North Atlantic are defined in the regions of  $50^{\circ}\text{N}$ - $75^{\circ}\text{N}$ ,  $60^{\circ}\text{W}$ - $10^{\circ}\text{E}$  and  $25^{\circ}\text{N}$ - $50^{\circ}\text{N}$ ,  $60^{\circ}\text{W}$ - $10^{\circ}\text{E}$ , respectively.

### Mean Streamfunction

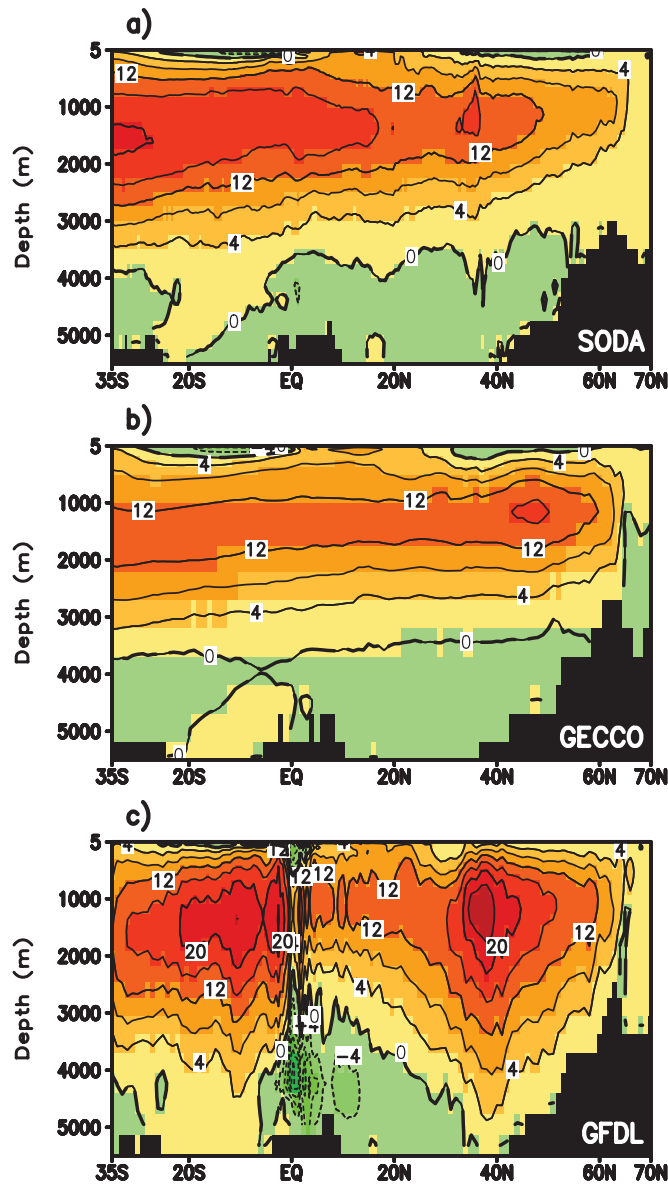


**Figure 14.** The mean streamfunction ( $S_v$ ) calculated from the (a) SODA, (b) GECCO, and (c) GFDL ocean reanalysis products. The AMOC is represented by a clockwise circulation cell consisting of an upper layer northward flow, a sinking flow in the northern high latitudes and a southward return flow at depth.

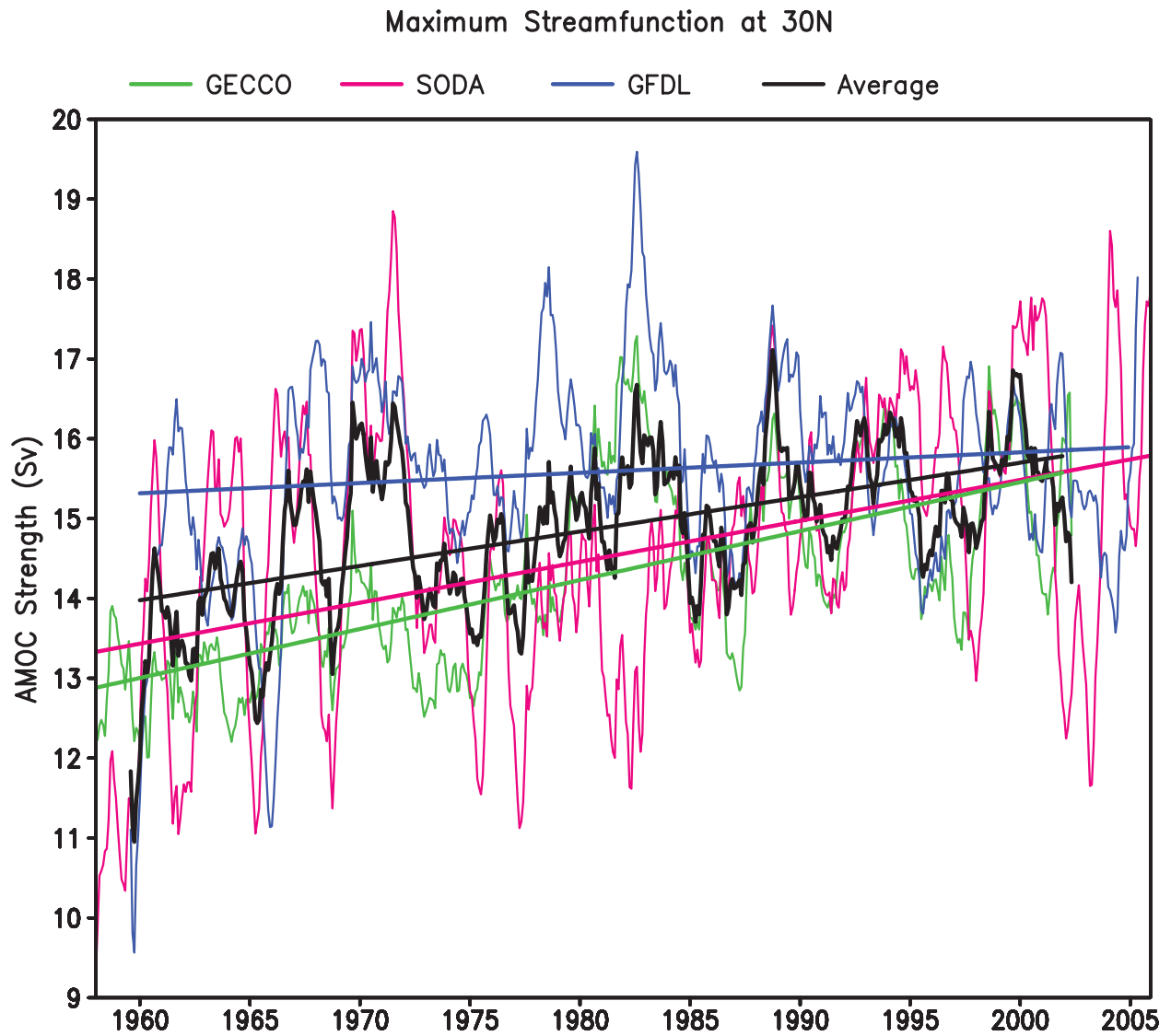


**Figure 15.** The time series of the maximum streamfunction (Sv) at 30°N from the SODA, GECCO, and GFDL ocean reanalysis products. The black curve is the ensemble average of three products. The straight lines are the linear trends that are fitted to their respective time series. An 11-month running mean is applied to the indices.

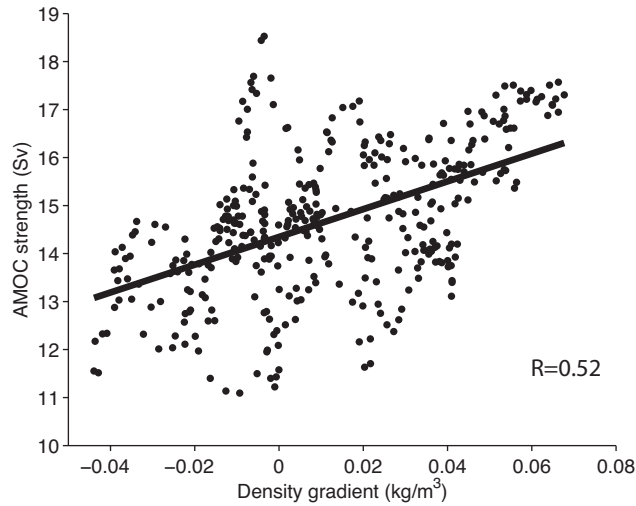


**Figure 16.** The scatter plot of the AMOC strength (Sv;  $1 \text{ Sv} = 10^6 \text{ m}^3/\text{s}$ ) versus the meridional potential density gradient ( $\text{kg}/\text{m}^3$ ) between the subpolar and subtropical North Atlantic Ocean, calculated from the SODA reanalysis from 1974-2005. The AMOC strength is measured by the maximum streamfunction at  $30^\circ\text{N}$ . The meridional potential density gradient is computed by the potential density anomaly (after removing seasonal cycle) difference between the regions of  $60^\circ\text{W}-10^\circ\text{W}$ ,  $52^\circ\text{N}-75^\circ\text{N}$  and  $70^\circ\text{W}-10^\circ\text{W}$ ,  $25^\circ\text{N}-50^\circ\text{N}$ . An 11-month running mean is applied to both indices before the scatter plot. The straight line represents the linear regression.